

Measurement of ground-penetrating radar antenna patterns using modulated scatterers

Ricardo A. López¹ and Waymond R. Scott, Jr.
School of Electrical and Computer Engineering, Georgia Institute of Technology
Atlanta, GA, 30332-0250, USA

ABSTRACT

The measurement of radiation patterns of antennas in air is relatively straightforward. In contrast, the measurement of the underground pattern for ground-penetrating radar (GPR) antennas poses particular challenges. Since GPRs are equipped with transmitting and receiving paths, the combined pattern is the most useful. To measure this pattern, a probe (scatterer) can be used to reflect part of the received signal back to the receiving antenna. However, the processing on the receiving end must determine whether or not that signal comes from the probe (“desired”) or from the soil or other objects (“undesired.”) These two issues can be addressed by using a modulated scatterer, i.e., a scatterer that is modulated at a frequency much less than the carrier frequency. The modulation can be realized either electrically or optically. The advantage of the optical approach is that spurious reflections are greatly reduced since an optical fiber is used instead of current-carrying metallic cables. The electrical approach, however, allows for deeper modulation levels, which increases the level of “desired” signal at the receiver. Another issue is related to the bandwidth of the scatterer. Since GPRs are generally very broadband, it is of interest to measure their broadband radiation patterns. The scatterers in the present work are successfully made broadband by resistively loading them. The results and trade-offs resulting from this technique are shown. In summary, the modulated scatterer technique is verified to be useful for these purposes. Experiments are realized in air and underground and the corresponding radiation patterns of a set of GPR antennas are shown.

Keywords: modulated scatterer, optically modulated scatterer, ground-penetrating radar.

1. INTRODUCTION

The measurement of the radiation pattern of an antenna in air does not present particular challenges when compared to the measurement of underground patterns for ground-penetrating radar antennas. First, since GPRs are equipped with transmitting and receiving paths (separate antennas or a single antenna that serves both purposes), the combined pattern is the most useful. If a probe is to be used to measure this pattern, it must be able to backscatter part of the radiated signal. An issue with this approach is the presence of inhomogeneities (clutter) in the ground. Some technique must be employed that differentiates reflections from these extraneous objects from those of the field probe. One such technique is to modulate the probe with a signal whose frequency is significantly less than the RF carrier frequency. This type of probe is known as a *modulated scatterer* (MS.) Typical devices to achieve the desired modulation are transistors and diodes. In our experiment, we use a microwave PIN diode in order to modulate the probe with electric current and a microwave PIN photodiode in order to modulate the probe with infrared light. While the electric modulation scheme reaches deeper levels of modulation, it also disrupts the field under test due to the use of metallic cables needed to bias the diode. On the other hand, the optical scheme uses a length of optical fiber, which minimizes field disruption, but the modulation level is not as large as in the electric case. It is important that the modulation be strong because it improves the signal-to-noise ratio.

¹rlopezm@ieee.org

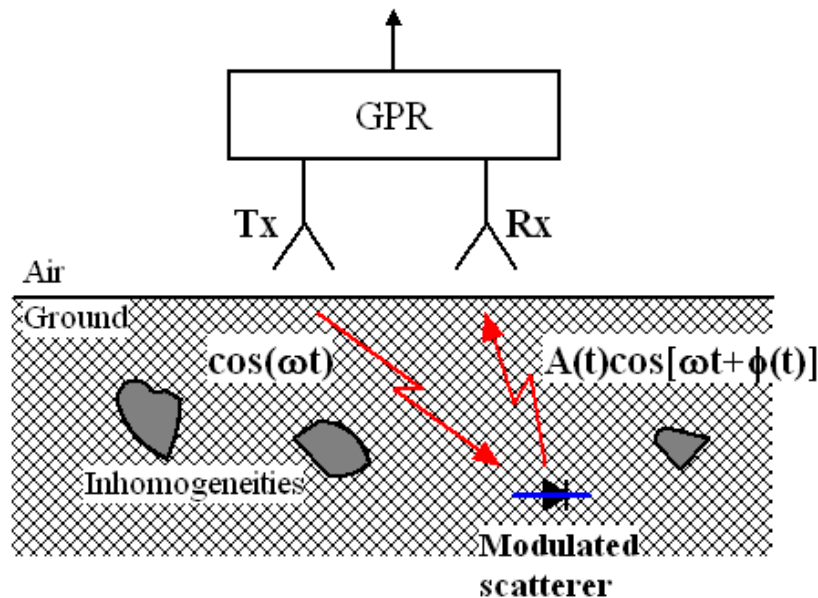


Figure 1. Diagram of the system used to measure underground patterns.

2. THEORETICAL BACKGROUND

Cullen and Parr [1] proved that the voltage received by a homodyne detector from a short dipole probe is approximately proportional to the square of the electric field along the probe:

$$V_r \propto (\vec{E} \cdot \vec{u}_l)^2$$

The square of the electric field, in the case of an antenna, effectively represents the two-way pattern of the radiator. If the cross-section of the probe is a function of time (as a result of modulating it, for example), then the received voltage will show an additional component that varies in time. Therefore, we are interested in measuring this time-varying component of V_r , ΔV_r , that varies in time at the same rate as the modulated probe does, which for the present experiment will be 30 kHz.

The received voltage contains modulated and unmodulated components and can be written, in general, as

$$V_r = [A + \Delta A(t)]\cos[\omega t + \varphi + \Delta\varphi(t)] + A_c\cos(\omega t + \varphi_c), \quad (1)$$

where A and φ account for unmodulated components in amplitude and phase, respectively, arising from the probe; and $\Delta A(t)$ and $\Delta\varphi(t)$ are the amplitude and phase modulation introduced by the modulated scatterer, respectively. A_c and φ_c are the amplitude and phase of the undesired coupling between the antennas, as well as reflections from the surroundings and clutter. If the probe were not modulated, its backscatter would be buried in this relatively large component, making it impossible to measure a good replica of the pattern.

A schematic diagram of the bistatic (separate transmitting and receiving antennas) homodyne radar system used in this work is shown in Figure 2. This radar was originally built to measure displacements of the surface of the earth and mines due to elastic waves [10] and it has been used here to perform the measurements described in Sections 4 and 5. Its operating frequency range is from 2 GHz to 8 GHz. The output of this radar consists of two baseband quadrature signals, obtained after the corresponding direct downconversion of the received RF signal.

Mathematically, if the transmitted RF carrier is a sinusoidal signal of the form $B\cos(\omega t)$, the outputs of the mixers can be expressed as (with V_r as in Equation 1; the “2” factors are used only for algebraic convenience and to avoid the use of fractional coefficients):

$$V_I = [2 \cos(\omega t)] \cdot V_r$$

$$V_Q = [-2 \sin(\omega t)] \cdot V_r$$

After some algebraic manipulation, and discarding the high-frequency components, the outputs are found to be

$$V_I \approx A \cos(\varphi) + A_c \cos(\varphi_c) + v_I(t)$$

$$V_Q \approx A \sin(\varphi) + A_c \sin(\varphi_c) + v_Q(t)$$

where $v_I(t)$ and $v_Q(t)$ are the time-varying components given by

$$v_I(t) = -A\Delta\varphi(t) \sin(\varphi) + \Delta A(t) \cos(\varphi)$$

$$v_Q(t) = \Delta A(t) \sin(\varphi) + A\Delta\varphi(t) \cos(\varphi)$$

An adequate measure of the intensity of the backscattered signal has been found to be simply

$$R = \sqrt{|v_I(t)|^2 + |v_Q(t)|^2} = |A| \sqrt{\left[\frac{\Delta A(t)}{A}\right]^2 + [\Delta\varphi(t)]^2} \quad (2)$$

In the remaining of this paper, the term *intensity of the modulated component* refers to R computed from the quadrature outputs of the GPR as shown in Equation 2.

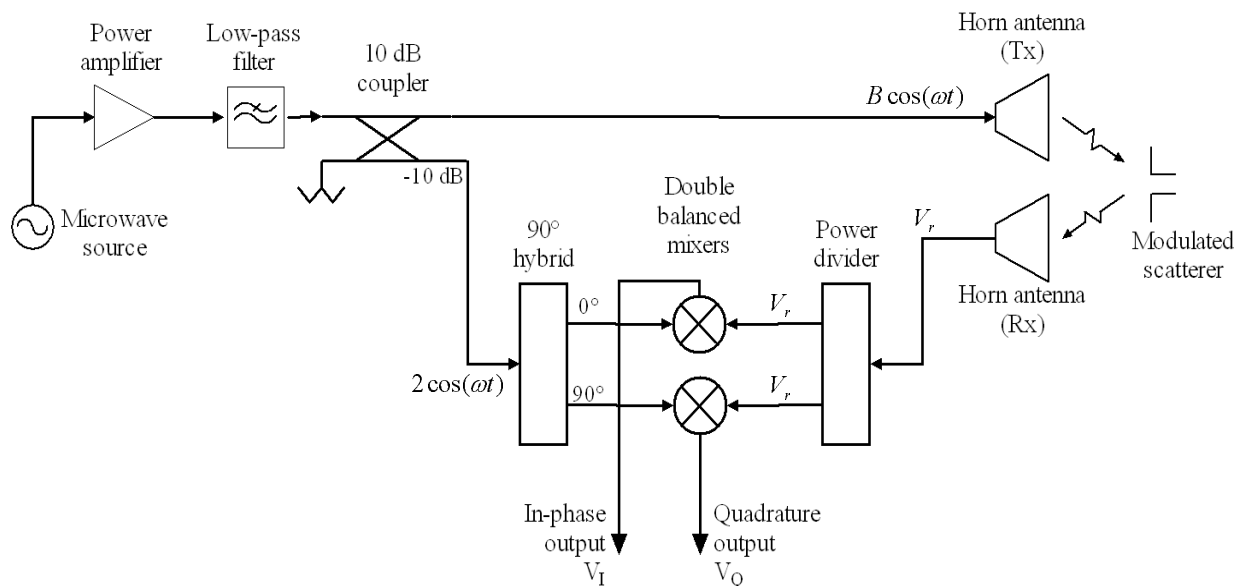


Figure 2. Block diagram of the homodyne radar system.

3. BANDWIDTH IMPROVEMENT

We choose to use a dipole probe, because it is relatively simple, small, and easy to build. The drawback of using a dipole as a probe is its frequency response. Since the dipole is a resonant structure, its response peaks at its resonant frequencies and therefore some technique to improve the bandwidth is required because GPRs are generally broadband devices. A possible solution is to shape the antenna so as to make it frequency independent [3]. However, this approach would require a larger probe, which would affect the field under test. A better solution is to resistively load the dipole, as proposed by Wu and King [4]. This method replaces the metallic arms of the probe by a conductive material whose resistivity per unit length (R_L) varies along the arms according to the profile shown in Equation 3, where the dipole is assumed to be centered at the origin and aligned along the z -axis, and where h represents the length of each of the arms. ψ is a parameter defined in [4].

$$R_L(z) = \frac{R_0}{1 - \left|\frac{z}{h}\right|}, \quad R_0 = \frac{\eta_0 \psi}{2\pi h} = 21766 \text{ } \Omega / m \quad (3)$$

For practical purposes, however, it is convenient to discretize Equation (3). In our experiments, the desired profile has been achieved by adding discrete surface mount (SMD) resistors along the arms of the dipoles, in series, at convenient distances from the center.

4. IMPLEMENTATION AND MEASUREMENTS IN AIR

In order to avoid significant disruption of the field under test, the modulating element must be small and symmetrical. Also, it must behave as closely to an ideal switch as possible (low impedance when turned on and high impedance when turned off.) In the case of the photodiode, its operating wavelength must be compatible with that of commercially available light sources, such as infrared (IR) LEDs. Finally, it must be easy to attach the optical fiber to the photodiode in an efficient way. After comparing PIN photodiodes from various manufacturers, the model FD80S7-F8 from Fermionics Inc. was chosen because of its small yet rugged layout and the fact that it comes already pigtailed with a length of $62.5\mu\text{m}/125\mu\text{m}$ optical fiber. The source of IR light was built using the IR LED AMP TYCO 259012-1. The system operates at a wavelength of $1.3 \mu\text{m}$. Photographs of the photodiode and the IR source are shown in Figure 3. The photodiode impedance was experimentally measured using a vector network analyzer over the frequency range 2 GHz to 8 GHz. It was found that IR LED currents above 60 mA did not provide further change in the photodiode impedance and, therefore, this value was taken as the threshold to turn the diode on. The photodiode's impedance was significantly less when it was illuminated by the LED than when the LED was off, i.e., the modulating capability of the device was confirmed.

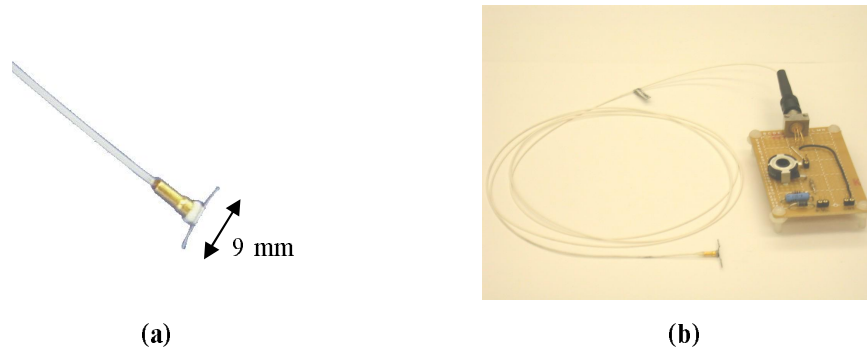


Figure 3. (a) The PIN photodiode FD80S7-F8, and (b) the IR source.

For the electrical version of the probes, the microwave PIN diode HPND 4005 (Agilent Technologies) was chosen. This device is very small (0.3 mm by 0.24 mm) and it has on and off resistances of 4.7Ω at 20 mA and more than $1k\Omega$ at cut-off, respectively. Hence, the “on” bias current was set at 20 mA.

In the remainder of this paper, the term *PEC probes* will refer to the probes with no resistive loading, and the term *Wu-King probes*, to the resistively-loaded ones. The following types of probes have been built on printed circuit boards (FR-4 material with 0.5 ounce copper foil):

4.1 Optical and electrical PEC probes

Optical (OMS) and electrical (EMS) versions of these probes were built. A photograph of the optical version can be seen in Figure 4. The EMS requires the addition of feeding lines to bias the PIN diode. The diode will be fed from a signal generator with a 30 kHz square signal via a pair of twisted wires. It is important to prevent RF leakage from the dipole into the wires and the signal generator. This has been achieved using a symmetrical first order low-pass RC network with a cutoff frequency of 1.5 MHz.

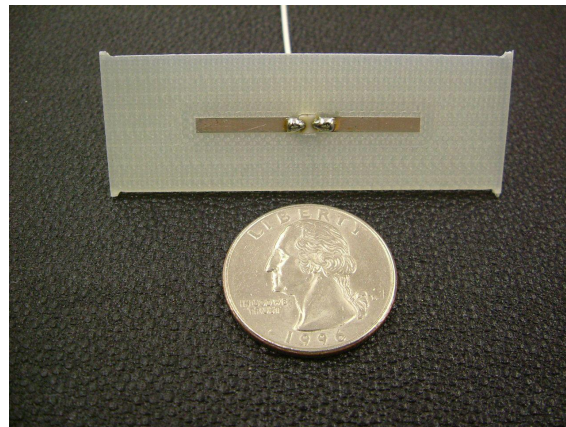


Figure 4. Optical PEC probe. Note the optical fiber leaving the probe from underneath it.

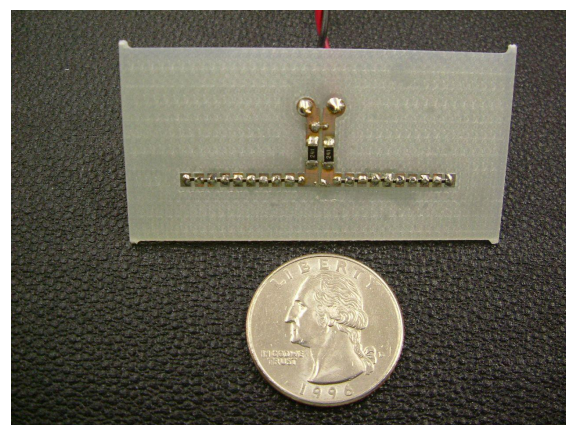


Figure 5. Electrical Wu-King probe, showing the low-pass feeding lines.

4.2 Optical and electrical Wu-King probes

The Wu-King probes are direct implementations of the discretized version of Equation 3, with the SMD resistors placed along the arms of the dipole. A photograph can be seen in Figure 5. The probe has a length of 4 cm. Eighteen resistive elements were used. The values of the resistors were chosen to be commercial values from 45.3Ω to 604Ω , with a tolerance of 2%.

4.3 Measurements in air

Preliminary experiments were run in order to assess the difference between the electrical and the optical probes. The intensity of the demodulated signal, R , is shown in Figure 6 when the modulated scatterers were located in front of a pair of horn antennas attached to the radar. Notice that, as expected, there is a difference in backscattering efficiency between the electrical and optical probes, with the former being 20 dB stronger than the latter. This is due to the inherently more ideal switching characteristic of the electrical PIN diodes. It is also observed that the resistively loaded probes show a more uniform frequency response, which serves to verify that the Wu-King technique works even for probes of this small size and with a relatively coarse discretization of the theoretical conductivity gradient. However, this uniformity comes at the price of less backscattering received from the Wu-King probes (by approximately 20 dB from 2 to 4 GHz,) due to the resistive loss introduced by the surface mounted resistors that make up the Wu-King profile. There is some discrepancy in the frequency response –particularly for the PEC probes– between these measured results and the previous simulations in [12]. This is believed to be caused by differences in the models for the PIN diode and PIN photodiode used in the simulations in [12], which becomes less accurate due to increased parasitic components as frequency increases. Notice that the peaks in response for both, PEC OMS and PEC EMS, happen at approximately the same range of frequencies (3 to 4 GHz,) as expected due to the geometry of the probes.

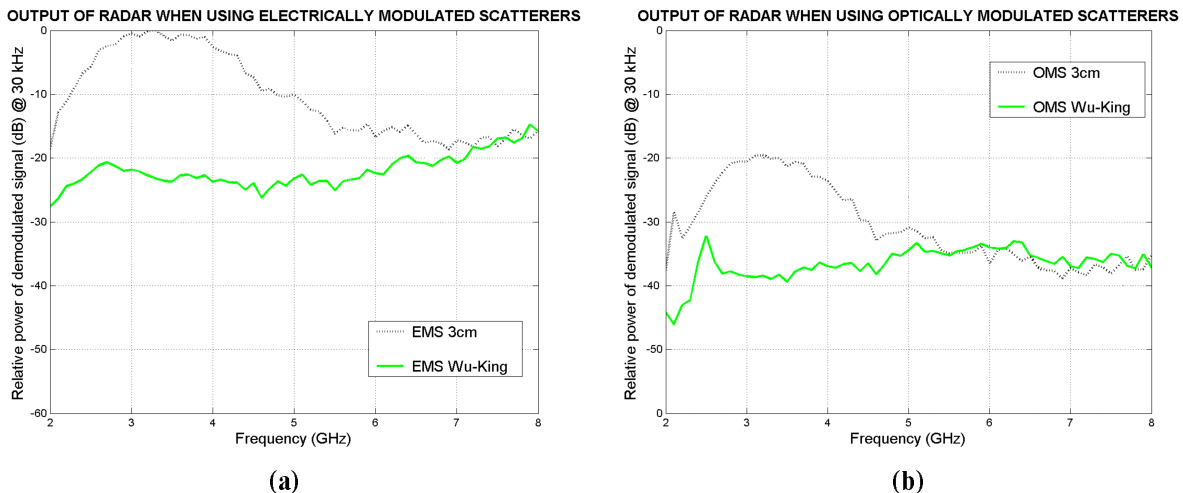


Figure 6. Measured output of the radar when using (a) electrically modulated scatterers (EMS,) and (b) optically modulated scatterers (OMS.)

5. UNDERGROUND MEASUREMENTS

The underground measurements were conducted in a sandbox testing facility, part of the Electromagnetics Laboratory at the School of Electrical Engineering at Georgia Tech. A pair of GPR antennas was scanned over an area of dimensions 1.0m x 1.0m. A computer-controlled XYZ positioning system was used to perform the scan. The same computer was in charge of data acquisition from the different instruments via the GPIB bus. The radar and the antennas were

The probes were buried at the center of the scanned area at a depth of 3 cm below the surface and were oriented parallel to the x-direction. The quadrature outputs of the radar were measured in order to compute the intensity of the backscattered modulated component as shown in Equation 2. In this experiment, the GPR radar was equipped with a pair of resistively-loaded, GPR vee antennas designed by Dr. Kangwook Kim [11]. A schematic of the setup can be seen in Figure 7. Figures 8 and 9 show the measured patterns when the electrical PEC, the electrical Wu-King, the optical PEC and the optical Wu-King probes described in Section 4 were used.

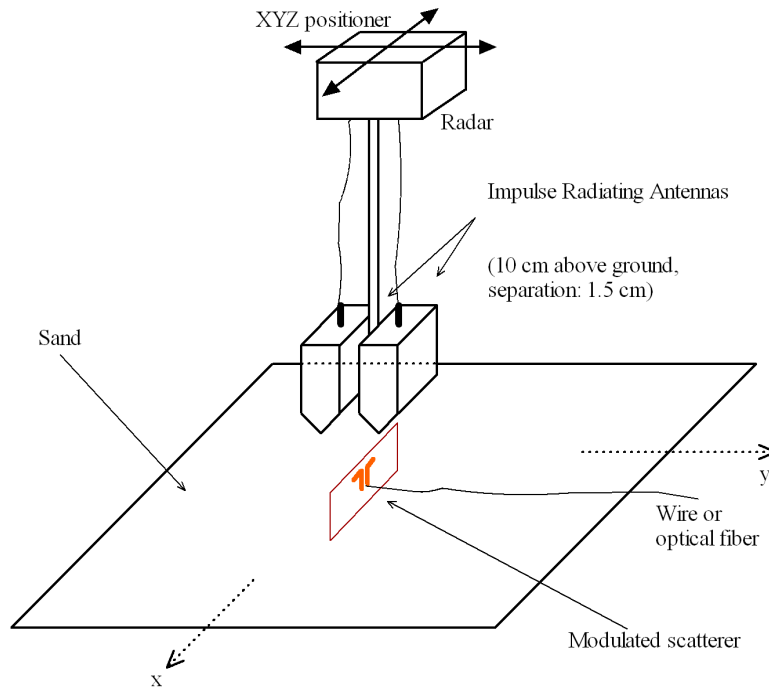


Figure 7. Schematic of the setup of the underground pattern measurement experiment.

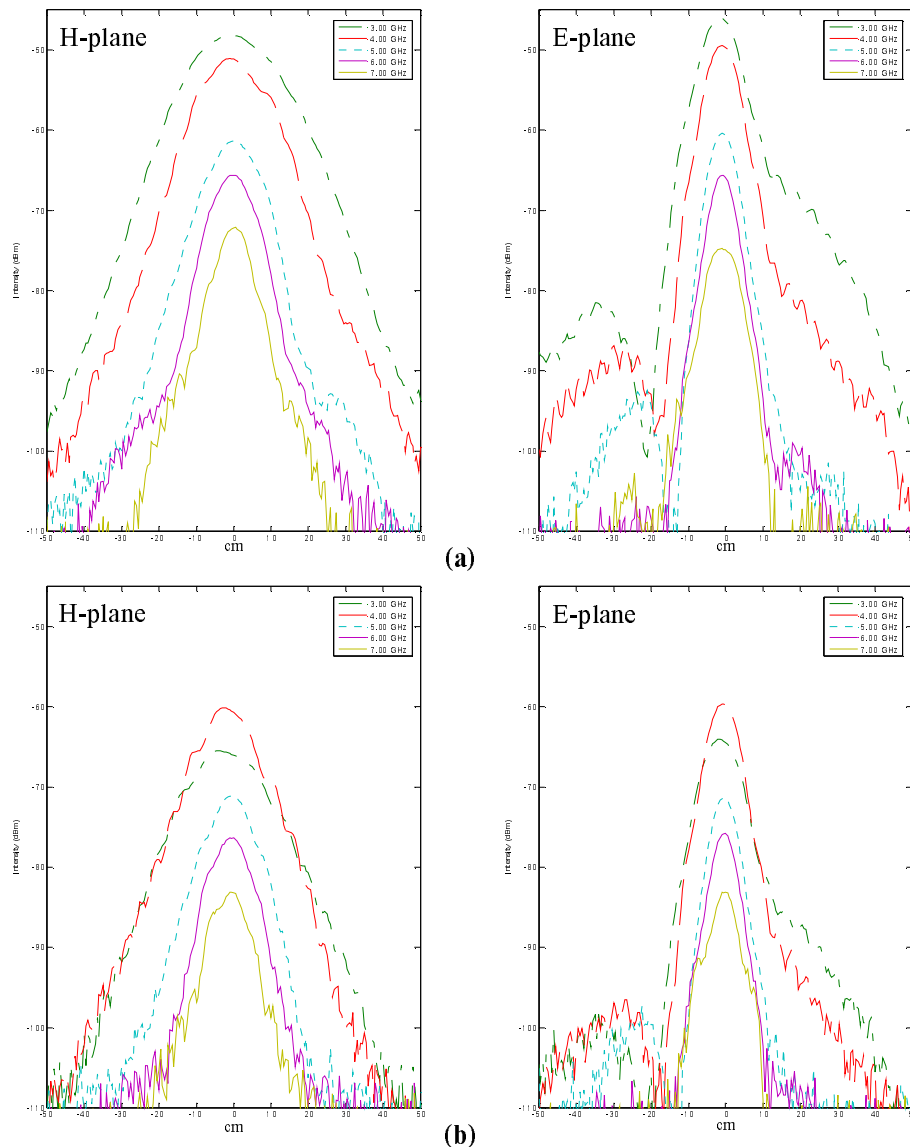


Figure 8. Measured patterns when (a) the electrical PEC, and (b) the optical PEC probes were buried 3 cm below the surface.

The patterns obtained using the PEC probes can be seen in Figure 8. The probes provide strong responses, and the electrical probe is approximately 13 dB stronger than the optical probe. They also show asymmetric patterns: the main lobe appears to be skewed to the right and even dominates the right sidelobe between 3 and 4 GHz at about 20 dB down the peak values. This phenomenon seems to be geometry- and frequency-related because it happens with the PEC probes but it is not seen with the Wu-King probes. Also, since the probes were not insulated, they may have been influenced by the varying degree of wetness of the surrounding sand, differences in contact with the sand along the body of the probe or even tilting of the probes after they were buried. However, this effect was not expected and deserves more investigation. Due to the irregular frequency response, it is seen that the spot size is not constant. For example, the 3-dB spot diameter varies between 6 cm and 25 cm, approximately, depending on the frequency.

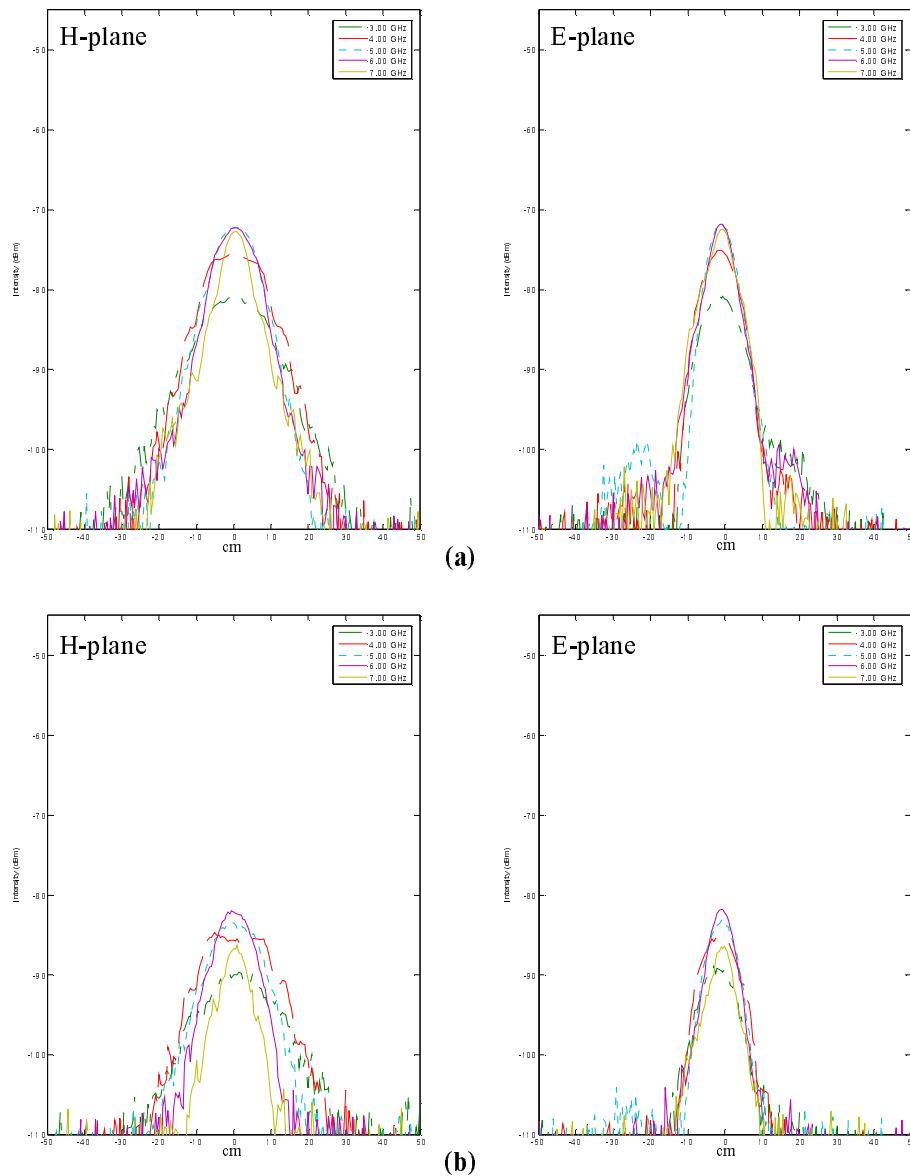


Figure 9. Pattern when (a) the electrical Wu-King, and (b) the optical Wu-King probes were buried 3 cm below the surface.

Figure 9 shows the patterns measured with the Wu-King probes. When comparing Figures 9 and 8, note the difference in response between the PEC and the Wu-King probes. The peaks of response are overall lower here, by approximately 20 dB (this is similar to the observed response when the measurements were made in air, as seen in Figure 6.) Also remarkable is the fact that the peaks are closer to each other, meaning that the frequency response is even more uniform with respect to Figure 8. Finally, the asymmetries observed with the PEC probes are not seen in these patterns. As a result of the more constant frequency response, the spot size appears smaller too, and the 3-dB spot diameter ranges, approximately, from 5 cm to 16 cm.

A summary of the underground measurements is shown in Figure 10, where the peak responses for the different probes at various frequencies are shown (four top curves, left-hand vertical axis.) There is a great degree of

similitude between these peak curves and the ones shown in Figure 6, the most notorious difference being that the probes backscatter more signal when they are not resistively loaded, the largest difference being approximately 35 dB at 3 GHz and no difference at 7.5 GHz. Similarly, the difference in response between corresponding electrical and optical probes in the mid-frequency range is constant and is about 10 dB. Likewise, the frequency response of the resistively loaded probes is flatter than their non-resistively loaded counterparts in the middle of the frequency range.

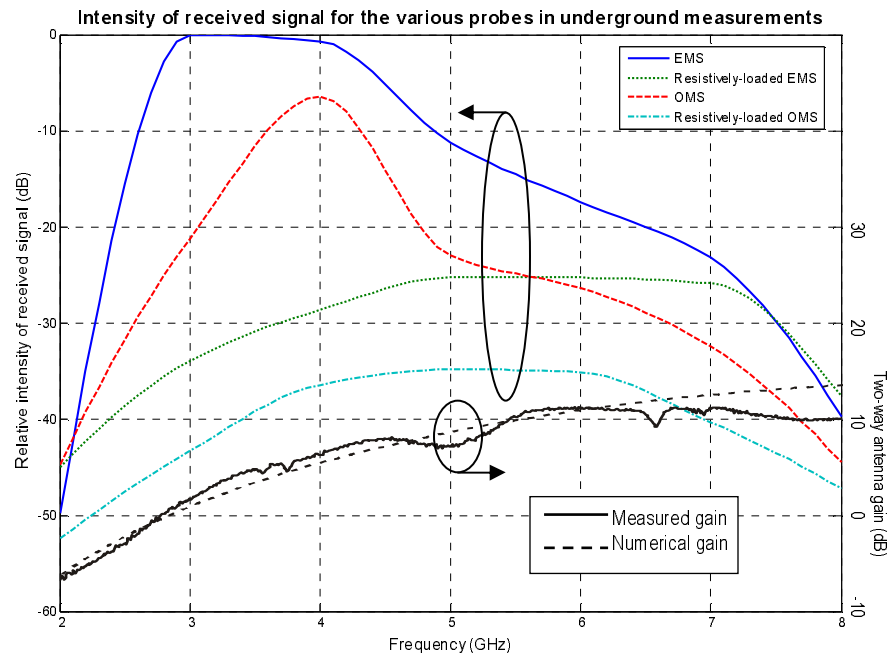


Figure 10. Relative intensity of the received signal for the different probes in the underground experiments vs. two-way gain of the Wu-King GPR vee antennas.

The two lower curves (right-hand side vertical axis) in Figure 10 show the two-way gain of the resistively-loaded vee antennas (measured and simulated) as found by Dr. Kangwook Kim using a different technique [13.] It is interesting to note that this gain profile is similar to the response plot obtained with the Wu-King probes in the present work. In particular, the gain roll-off at the lower frequency end is remarkably similar. There is a difference at the upper frequency range, though, which is believed to be due to the frequency response of the modulating element and the fact that the radar is approaching its upper limit of operation (8 GHz.) This difference will be further investigated.

6. CONCLUSIONS AND FUTURE WORK

We have been able to successfully use modulated scatterers to measure in-air and underground patterns. It is clear that the most challenging feature to optimize is the pattern bandwidth. The problem of non-uniform frequency response was solved by resistively loading the probe according to the Wu-King theory, at the expense of backscattering efficiency. This loss in radar cross section was particularly critical in the case of the optical probes and future work is aimed toward improving the corresponding radar cross section. Also, the asymmetries observed

in the patterns will be further investigated by performing additional measurements at selected frequencies. The gain calibration of the system is also important and will be addressed. The probes used in this experiment were not insulated; therefore, underground measurements using insulated probes will be carried out. A new radar that can work at frequencies below 2 GHz will be built and used to carry out measurements at lower frequencies. Last but not least, it is of interest to measure the polarization features of GPR antennas and techniques will be investigated and implemented in order to measure such features.

ACKNOWLEDGEMENTS

This work is supported by the US Army Night Vision and Electronic Sensors Directorate, Science and Technology Division, Countermines Branch. We would like to thank Mr. Gregg Larson for his help with the XYZ positioning system and the use of the sandbox facility, as well as Dr. Kangwook Kim for providing some helpful insight and data from his experiments.

REFERENCES

1. A. M. Cullen and J. C. Parr, "A new perturbation method for measuring microwave fields in free space," *Proc. IEE*, vol. 102b, pp. 836-844, 1955.
2. J. C. Bolomey and F. E. Gardiol, *Engineering Applications of the Modulated Scatterer Technique*. Norwood, MA: Artech House, 2001.
3. C. A. Balanis, *Antenna Engineering*. New York, NY: John Wiley & Sons, 1997.
4. T. T. Wu and R. W. P. King, "The cylindrical antenna with nonreflecting resistive loading," *IEEE Transactions on Antennas and Propagation*, vol. AP-13, pp. 369-373, May 1965.
5. D. Slater, *Near-Field Antenna Measurements*. Norwood, MA: Artech House, 1991.
6. G. Hygate and J. F. Nye, "Measuring microwave fields directly with an optically modulated scatterer," *Measurement Science and Technology*, vol. 1, pp. 703-709, 1990.
7. Fermionics, Inc., "Type S7 Package (High Speed Mini-Pigtail) [p/n FD80S7-F]." [Online document], 2003, Available HTTP: <http://www.fermionics.com/S7pic.htm>.
8. Seung-Ho Lee, *Measurement of Time-Varying Surface Displacements using a Radar*. Doctoral Thesis in Electrical and Computer Engineering, Georgia Institute of Technology, Atlanta, GA, 2002.
9. D. M. Pozar, *Microwave Engineering*. New York, NY: John Wiley & Sons, 1998.
10. W. R. Scott, Jr., C. T. Schröder and J. S. Martin, "An acousto-electromagnetic sensor for locating land mines," *Detection and Remediation Technologies for Mines and Minelike Targets III, Proc. SPIE*, April 1998, vol. 3392, pp. 176-186.
11. K. Kim, A. C. Gurbuz, W. R. Scott, Jr. and J. H. McClellan, "A multistatic ground-penetrating radar with an array of resistively-loaded vee dipole antennas for landmine detection," to be presented at the *Detection and Remediation Technologies for Mines and Minelike Targets X Conference, SPIE Defense and Security Symposium*, March 2005.
12. Ricardo A. Lopez and W. R. Scott, Jr., "Investigation of the suitability of using modulated scatterers to measure the pattern of ground-penetrating radar antennas," *Detection and Remediation Technologies for Mines and Minelike Targets IX, Proc. SPIE*, April 2004, vol. 5415, pp. 371-382.
13. K. Kim and W. R. Scott, Jr., "A resistive linear antenna for ground-penetrating radars," *Detection and Remediation Technologies for Mines and Minelike Targets IX, Proc. SPIE*, April 2004, vol. 5415, pp. 359-370.